Earthquake Engineering & Structural Dynamics
The Journal of the International Association for Earthquake Engineering

EARTHQUAKE ENGINEERING & STRUCTURAL DYNAMICS
Earthquake Engng Struct. Dyn. 2013; **42**:1203–1219
Published online 29 October 2012 in Wiley Online Library (wileyonlinelibrary.com). DOI: 10.1002/eqe.2267

A probabilistic performance-based approach for mitigating the seismic pounding risk between adjacent buildings

M. Barbato[1,*,†] and E. Tubaldi[2]

[1]*Department of Civil and Environmental Engineering, Louisiana State University and A&M College, 3531 Patrick F. Taylor Hall, Nicholson Extension, Baton Rouge, LA 70803, USA*
[2]*School of Architecture and Design, University of Camerino, Viale della Rimembranza, Ascoli Piceno, 63100, Italy*

ABSTRACT

Existing design procedures for determining the separation distance between adjacent buildings subjected to seismic pounding risk are based on approximations of the buildings' peak relative displacement. These procedures are characterized by unknown safety levels and thus are not suitable for use within a performance-based earthquake engineering framework.

This paper introduces an innovative reliability-based methodology for the design of the separation distance between adjacent buildings. The proposed methodology, which is naturally integrated into modern performance-based design procedures, provides the value of the separation distance corresponding to a target probability of pounding during the design life of the buildings. It recasts the inverse reliability problem of the determination of the design separation distance as a zero-finding problem and involves the use of analytical techniques in order to evaluate the statistics of the dynamic response of the buildings. Both uncertainty in the seismic intensity and record-to-record variability are taken into account.

The proposed methodology is applied to several different buildings modeled as linear elastic single-degree-of-freedom (SDOF) and multi-degree-of-freedom (MDOF) systems, as well as SDOF nonlinear hysteretic systems. The design separation distances obtained are compared with the corresponding estimates that are based on several response combination rules suggested in the seismic design codes and in the literature. In contrast to current seismic code design procedures, the newly proposed methodology provides consistent safety levels for different building properties and different seismic hazard conditions. Copyright © 2012 John Wiley & Sons, Ltd.

Received 4 December 2011; Revised 1 June 2012; Accepted 1 October 2012

KEY WORDS: seismic pounding; separation distance; performance-based earthquake engineering; design procedure; nonstationary random processes; inverse reliability problem

1. INTRODUCTION

Seismic pounding between adjacent buildings is an undesirable phenomenon that can cause severe damage to the colliding buildings. In order to mitigate the risk of seismic pounding between new buildings, current seismic design codes [1–4] prescribe a minimum separation distance (often referred to as critical separation distance (CSD)) between adjacent structures. The value of the CSD is assumed equal to the peak relative displacement computed at the most likely pounding location and corresponding to a site-specific seismic intensity. This site-specific seismic intensity is usually defined using a uniform-hazard response spectrum, whose spectral ordinates are characterized by a target return period. For example, according to Eurocode 8 [4], the pounding event corresponds to an ultimate limit

*Correspondence to: M. Barbato, Department of Civil and Environmental Engineering, Louisiana State University and A&M College, 3531 Patrick F. Taylor Hall, Nicholson Extension, Baton Rouge, LA, 70803, USA.
†E-mail: mbarbato@lsu.edu

state condition, and the CSD is determined for the earthquake intensity having a return period of 475 years, corresponding to a probability of exceedance of 10% in 50 years.

Given the seismic input, the peak relative displacement is obtained from the values of the peak displacements of the two adjacent buildings, which can be calculated using various structural analysis techniques (e.g., spectral analysis, pushover analysis, and time-history analysis). Simplified response combination rules (e.g., the absolute sum (ABS) rule and the square-root-of-the-sums-of-squares (SRSS) rule) are then employed to derive the peak relative displacement U_{rel} between buildings A and B, as a function of their absolute peak displacements $U_{\text{rel,A}}$ and $U_{\text{rel,B}}$. These approximate response combination rules neglect the phase differences between the dynamic responses of the adjacent structures. In order to overcome this drawback, the use of the double difference combination (DDC) rule for determining the CSD has been proposed and investigated by several authors for elastic single-degree-of-freedom (SDOF) systems [5–8] and then extended to elastic multi-degree-of-freedom (MDOF) systems [5] and to nonlinear systems (see [9] for a state-of-the-art of the available techniques).

Despite the research advances in estimating the CSD, the approach currently employed in the seismic codes and based on the use of approximate response combination rules presents many limits and shortcomings. First, unless time-history analysis is employed to estimate the peak displacement responses of the buildings, the response combination rules can employ only the peak displacements corresponding to a double-barrier reliability problem [8, 10, 11], whereas the seismic pounding problem is a single-barrier reliability problem (i.e., seismic pounding happens only when the two adjacent buildings vibrate toward each other and not when they move away from each other). In addition, the code approach for the CSD design can be inaccurate for MDOF systems whose response receives a significant contribution from several vibration modes and/or exhibits large inelastic deformations [9]. An even more serious limitation of the current design approach is that the building separation distances obtained are characterized by unknown safety levels, which strongly depend on the natural periods of the adjacent buildings [8–12]. Furthermore, the design of the CSD is performed for a single hazard level (by employing uniform hazard spectra), neglecting any other information on the seismic hazard of the building site [13]. Therefore, the current CSD design approach does not permit the designer to quantify and control directly the structural performance and the reliability of the design [13–16] and does not provide a sound basis for the development of earthquake risk management strategies [16].

This study proposes a new reliability-based methodology for the definition of the separation distance between adjacent buildings. This methodology overcomes the aforementioned limitations of the current CSD design approach by finding the separation distance that corresponds to a target value of the pounding probability during the building design life for a continuum of hazard levels. It accounts rigorously for all pertinent sources of uncertainty and properly treats the seismic pounding problem as a single-barrier reliability problem. Thus, it allows the designer to rationally choose a CSD that ensures consistent safety levels for different types of structures and to directly control and mitigate the consequences of damage due to pounding. The proposed design methodology is conceptually similar to other modern approaches that enforce explicit performance objectives in terms of target reliability and that are currently being developed in several areas of seismic and structural engineering [17–19].

The design of the CSD between adjacent buildings corresponding to a target value of the probability of pounding during the building design life is a typical inverse reliability problem [19, 20]. The corresponding direct reliability problem (i.e., the estimation of the pounding probability for a given value of the separation distance) has been recently studied in Tubaldi *et al*. [10, 11], where a probabilistic assessment methodology has been proposed within the context of modern performance-based earthquake engineering frameworks, such as the Pacific Earthquake Engineering Research Center framework [21, 22].

In this study, the design of the CSD is performed by recasting the inverse reliability problem described above as a zero-finding problem. Different solution algorithms are proposed and compared in terms of accuracy and computational cost. The capabilities of the proposed methodology are illustrated by considering the design of the separation distance between buildings modeled as linear elastic systems subjected to Gaussian excitations. This specialization takes advantage of existing efficient analytical [23–25] and/or stochastic simulation techniques [26] for estimating the reliability of seismically excited linear buildings with classical and nonclassical damping. It is also important because it allows to (i) provide a comparison with, and highlight the limitations of, current CSD

DOI: 10.1002/eqe

design methodologies, (ii) perform useful and extensive parametric analyses to understand the effects of different variables on the probability of pounding and the CSD, and (iii) develop efficient algorithms for the solution of the CSD design problem based on linear structural models that are often employed by practicing engineers. The extension of the proposed design methodology to nonlinear systems is also briefly illustrated. Because of space constraints and for the sake of clarity, only the seismic input uncertainty is explicitly taken into account, whereas the uncertainty affecting the parameters describing the structural models, albeit important [11], is not considered here. It is noted that the effects of model parameter uncertainty can be easily included in the proposed design methodology at the expense of an increased computational effort.

2. PERFORMANCE-BASED DETERMINATION OF THE CRITICAL SEPARATION DISTANCE

In this section of the paper, both the direct and inverse reliability problems (i.e., the seismic pounding probability assessment for given building properties and separation distance, and the design of the CSD distance for a given target pounding probability, respectively) are formalized mathematically. A brief review of the solution for the direct reliability problem is provided. Finally, several algorithms for the solution of the inverse reliability problem are proposed and illustrated.

2.1. Direct reliability problem: seismic pounding risk assessment

The direct reliability problem [11] consists of computing the probability, $P_{\mathrm{p}}(\xi,t_{\mathrm{L}})$, that the relative displacement between adjacent buildings, U_{rel}, out-crosses their separation distance, ξ, at least once over their design life, t_{L}. Assuming that the occurrence of a pounding event can be described by a Poisson process and that the buildings are immediately restored to their original condition after pounding occurrence, the value of $P_{\mathrm{p}}(\xi,t_{\mathrm{L}})$ can be computed as [11, 27]

$$P_{\mathrm{p}}(\xi, t_{\mathrm{L}}) = 1 - e^{-\nu_{\mathrm{p}}(\xi)\cdot t_{\mathrm{L}}} \tag{1}$$

in which $\nu_{\mathrm{p}}(\xi)$ is the mean annual frequency of pounding, which is computed as

$$\nu_{\mathrm{p}}(\xi) = \int_{im} P_{\mathrm{p}|IM(\xi)}\cdot|\mathrm{d}\nu_{IM}(im)| \tag{2}$$

where $P_{\mathrm{p}|IM}(\xi)$ is the probability of pounding conditional to the seismic intensity $IM = im$ and $\nu_{IM}(im)$ is the mean annual frequency of exceedance of a specific value im of the seismic intensity IM. In [11], the site peak ground acceleration (PGA) is employed as IM.

The conditional failure probability $P_{\mathrm{p}|IM}(\xi)$ is the solution of the following single-barrier first-passage reliability problem:

$$P_{\mathrm{p}|IM}(\xi) = P\left\{\max_{0\leqslant t\leqslant t_{\max}}[U_{\mathrm{rel}}(t)]\geqslant\xi|IM = im\right\} \tag{3}$$

in which t denotes time, $t_{\max}$ is the duration of the seismic excitation, $U_{\mathrm{rel}}(t) = U_{\mathrm{A}}(t) - U_{\mathrm{B}}(t)$, $U_{\mathrm{A}}(t)$ and $U_{\mathrm{B}}(t)$ are the displacement responses of buildings A and B at the most likely pounding location (usually identified as the roof level of the lower building, see Figure 1).

Tubaldi *et al*. [11] have proposed a methodology for assessing the seismic pounding risk between linear elastic models of adjacent buildings with deterministic and/or uncertain properties, which are subjected to Gaussian excitations. This methodology employs an efficient combination of simulation and analytical techniques and is based on existing exact closed-form solutions for the statistics of the buildings' displacement response processes [23, 24]. Several analytical approximations available in the literature (i.e., the Poisson's (P), the classical Vanmarcke's (cVM), and the modified Vanmarcke's (mVM) approximation) have been compared in terms of their accuracy in estimating

DOI: 10.1002/eqe

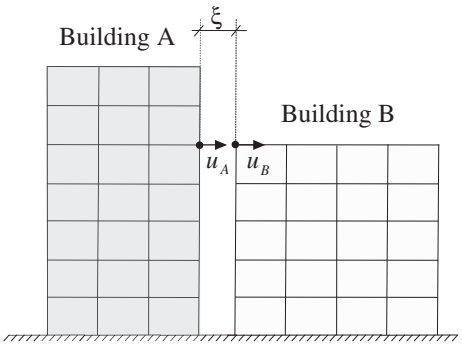

Figure 1. Geometric description of the pounding problem between adjacent buildings.

the conditional pounding probability $P_{p|IM}(\xi)$. The efficient importance sampling using elementary events (ISEE) method [26] has been employed to obtain a reference solution and to check the accuracy of these analytical techniques. Consistently with other recent studies [25, 28, 29], it has been found that the cVM and mVM approximations are, in general, more accurate than the P approximation. In addition, these three analytical approximations are more accurate when the natural periods T_A and T_B of the two adjacent structural systems are well separated than when these natural periods have similar values.

If the buildings are expected to exhibit significant inelastic deformations before pounding, the methodology presented in [11] can still be used. However, the nonlinear structural behavior must be taken into account by using appropriate analytical (e.g., stochastic linearization [30]) or simulation techniques (e.g., crude Monte Carlo simulation [9, 27] and subset simulation [31]) for evaluating $U_{rel}(t)$ in Equation (3). Thus, the computational cost of evaluating Equation (1) can significantly increase with the complexity of the nonlinear structural model considered.

2.2. *Inverse reliability problem: determination of the critical separation distance*

The inverse reliability problem corresponding to the determination of the CSD can be expressed as follows:

$$\text{Find } \xi^* \text{ such that } \quad P_p(\xi^*, t_L) = \bar{P}_p \tag{4}$$

where ξ^* is the separation distance corresponding to the target failure probability $\bar{P}_p$.

No analytical solution is currently available for the problem defined by Equation (4). A naive procedure for finding an approximate solution consists in solving the direct reliability problem given in Equation (1) for several discrete values of the separation distance ξ. The design separation distance is approximated by the value of ξ for which the pounding probability is closest to the target value. The range for the values of ξ could be decided on the basis of experience or on approximate estimates of the minimum separation distance suggested in current seismic codes. This heuristic approach is computationally expensive, potentially inaccurate, and difficult to generalize and/or automate.

The methodology proposed in this paper overcomes the drawbacks of the heuristic approach by recasting the inverse reliability problem of Equation (4) as the following zero-finding problem:

$$\xi^* = \text{Zero}[f(\xi)] \tag{5}$$

where the functional expression Zero[...] denotes the zero of the function in the parentheses and function $f(\xi)$ is defined as

$$f(\xi) = P_p(\xi, t_L) - \bar{P}_p \tag{6}$$

Function $f(\xi)$ is monotonically decreasing for increasing ξ, because the pounding probability decreases as the separation distance increases. Thus, $f(\xi)$ has a unique zero that coincides with the

DOI: 10.1002/eqe

desired solution ξ^* of the inverse reliability problem defined in Equation (4). This zero-finding problem can be solved using classical iterative optimization algorithms [32] such as the bisection method or gradient-based algorithms, which are usually more efficient. In this study, three different algorithms based on the safeguarded Newton's method [32] are proposed for estimating the CSD ξ^* (i.e., for solving Equation (5)). The safeguarded Newton's method is a hybrid zero-finding method that uses a Newton's (or quasi-Newton's) iteration while maintaining an interval containing the root of the function as in the bisection method. If the Newton's iteration falls outside this interval, the method switches to bisection for that iteration and then continues with Newton's method for the next iteration. The safeguarded Newton's algorithm is employed for its fast convergence rate and robustness. The three proposed solution algorithms differ in the strategy adopted to estimate $P_{\mathrm{pl}IM}(\xi)$ and its gradient at each iteration of the safeguarded Newton's method, and are characterized by a different level of accuracy and computational cost.

2.3. Proposed solution algorithms

The first solution algorithm (referred to as analytical (AN) algorithm) is purely analytical and uses analytical approximate solutions of $P_{\mathrm{pl}IM}(\xi)$ (i.e., P, cVM, or mVM approximations) to estimate $f(\xi)$ and its first derivative $f'(\xi) = \mathrm{d}f(\xi)/\mathrm{d}\,\xi$. The latter quantity is computed by forward finite difference numerical differentiation, using analytical estimates of $f(\xi)$ and $f(\xi + \Delta\xi)$, where $\Delta\xi$ denotes a small but finite increment of ξ. The starting point for the AN algorithm can be chosen, for example, as the CSD provided by the DDC rule for the value of the *IM* corresponding to the target return period. It is noteworthy that the performance of the AN algorithm is only slightly affected by the algorithm's starting point for any reasonable initial estimate of the CSD. The estimate of ξ^* obtained using the AN algorithm is denoted as ξ^*_{AN}.

The second solution algorithm (referred to as simulation (SIM) algorithm) employs a random simulation technique to estimate both $f(\xi)$ and $f'(\xi)$. The latter quantity is computed by forward finite difference numerical differentiation, using random simulation estimates of $f(\xi)$ and $f(\xi + \Delta\xi)$. The starting point of the SIM algorithm is taken as the solution of the AN algorithm, ξ^*_{AN}. The estimate of ξ^* obtained using the SIM algorithm is denoted as ξ^*_{SIM}.

The third solution algorithm proposed in this study (referred to as hybrid (HYB) algorithm) combines analytical and simulation techniques to improve the accuracy of the AN algorithm in estimating ξ^*. The HYB algorithm employs a random simulation technique to evaluate $f(\xi)$ and an analytical approximation for computing $f'(\xi)$ by forward finite difference. In particular, $f'(\xi)$ is computed using analytical estimates of $f(\xi)$ and $f(\xi + \Delta\xi)$. The starting point of the HYB algorithm coincides with the solution of the AN algorithm, ξ^*_{AN}. The estimate of ξ^* obtained using the HYB algorithm is denoted as ξ^*_{HYB}.

All three iterative algorithms presented earlier are terminated when the absolute value of $f(\xi)$ becomes smaller than a user-defined level of accuracy δ_f. It is noteworthy that analytical approximations of $P_{\mathrm{pl}IM}(\xi)$ result in a continuous smooth function $f(\xi)$ and an accurate estimate of its first derivative, which ensures a fast convergence of the iterative zero-finding procedure. On the other hand, the use of stochastic simulation techniques requires a very accurate estimate of $f(\xi)$ and $f(\xi + \Delta\xi)$ (i.e., a very small coefficient of variation for the estimates of $P_{\mathrm{pl}IM}(\xi)$ and $P_{\mathrm{pl}IM}(\xi + \Delta\xi)$, respectively) in order to obtain an estimate of the first derivative $f'(\xi)$ that is sufficiently accurate to ensure convergence of the zero-finding algorithm, thus resulting in a high computational cost for each evaluation of $f(\xi)$ and $f'(\xi)$.

In this study, the three proposed solution algorithms are illustrated and compared using the assumptions that the seismic loading is represented by Gaussian processes and that the structural behavior of the buildings is linear elastic before pounding. The latter assumption is widely used for design purposes and is consistent with the procedures suggested in current seismic design codes for estimating the CSD between adjacent buildings. Under the aforementioned assumptions, the P, cVM, and mVM analytical approximations can be computed in closed-form [23–25], whereas the ISEE method [26] can be employed as an efficient simulation technique to estimate $P_{\mathrm{pl}IM}(\xi)$. It is noteworthy that the proposed solution algorithms can also be applied to the cases of nonlinear structural behavior and non-Gaussian input excitations. In particular, the nonlinear structural

DOI: 10.1002/eqe

behavior can be included by using appropriate techniques to compute $P_{\mathrm{pl}|IM}(\xi)$, e.g. stochastic linearization, crude Monte Carlo, and subset simulation [9, 27, 30, 31]. Since these techniques are more expensive computationally than analytical solutions and ISEE for linear elastic problems, the computational cost of the proposed algorithms increases for nonlinear inelastic structural models. In this study, the application of the proposed methodology to nonlinear hysteretic systems is illustrated using the SIM algorithm in conjunction with crude Monte Carlo simulation for evaluating $f(\xi)$ and $f'(\xi)$. The combination of analytical random vibration techniques and efficient stochastic simulation methods for the computationally efficient solution of the problem defined by Equation (4) in the case of nonlinear inelastic structural systems is a very important and challenging task. However, it is out of the scope of this study, which focuses on the development of the performance-based CSD design framework.

3. APPLICATION EXAMPLES

In this section, the computational cost and accuracy of the proposed algorithms is compared by analyzing two different sets of adjacent buildings modeled as SDOF systems with close and well-separated periods of vibration. On the basis of the results obtained from this comparison, the techniques with the best compromise between accuracy and computational efficiency are selected and employed in an extensive parametric study that compares, for a wide range of vibration periods of the two SDOF systems and different seismic hazard conditions, the separation distances computed according to both the procedure recommended in the design codes and the newly proposed reliability-based technique. Then, the case of two adjacent buildings modeled as MDOF systems is analyzed in order to illustrate the capability of the proposed technique to deal with more complex systems. Finally, the proposed CSD design methodology is applied to adjacent buildings modeled as SDOF nonlinear hysteretic systems considering a wide range of values of the parameters describing the nonlinearity of the systems. The CSD values obtained are compared with those corresponding to simplified design procedures available in the literature.

3.1. Seismic input description and hazard model

In all the application examples considered here, the input ground acceleration is modeled by a time-modulated Gaussian process. The time-modulating function, $I(t)$, is represented by the Shinozuka–Sato's function [33], i.e.,

$$I(t) = c\cdot\left(e^{-b_1\cdot t} - e^{-b_2\cdot t}\right)\cdot H(t) \tag{7}$$

in which $b_1 = 0.045\pi$ s^{-1}, $b_2 = 0.050\pi$ s^{-1}, $c = 25.812$, and $H(t)$ is a unit step function. A duration $t_{\max} = 30$ s is considered for the seismic excitation.

The PSD of the embedded stationary process is described by the widely used Kanai–Tajimi model, as modified by Clough and Penzien [34], i.e.,

$$S_{\mathrm{CP}}(\omega) = S_0\cdot\frac{\omega_{\mathrm{g}}^4 + 4\cdot\xi_{\mathrm{g}}^2\cdot\omega^2\cdot\omega_{\mathrm{g}}^2}{\left[\omega_{\mathrm{g}}^2 - \omega^2\right]^2 + 4\cdot\xi_{\mathrm{g}}^2\cdot\omega^2\cdot\omega_{\mathrm{g}}^2}\cdot\frac{\omega^4}{\left[\omega_{\mathrm{f}}^2 - \omega^2\right]^2 + 4\cdot\xi_{\mathrm{f}}^2\cdot\omega^2\cdot\omega_{\mathrm{f}}^2} \tag{8}$$

in which S_0 denotes the amplitude of the bedrock excitation spectrum, modeled as a white noise process; ω_{g} and ξ_{g} are the fundamental circular frequency and damping factor of the soil, respectively; and ω_{f} and ξ_{f} are the parameters describing the Clough–Penzien filter. The values of the parameters employed for all the applications are $\omega_{\mathrm{g}} = 12.5$ rad/s, $\xi_{\mathrm{g}} = 0.6$, $\omega_{\mathrm{f}} = 2$ rad/s, and $\xi_{\mathrm{f}} = 0.7$. The PSD function in Equation (8) is shown in Figure 2(a) for $S_0 = 1$ m^2/s^3.

The peak ground acceleration, *PGA*, is assumed here as *IM*. It is noteworthy that the proposed methodology is independent of the choice of the *IM*. In order to derive the fragility curves in terms of the selected *IM*, the relationship between the parameter S_0 of the Kanai–Tajimi spectrum and the

DOI: 10.1002/eqe

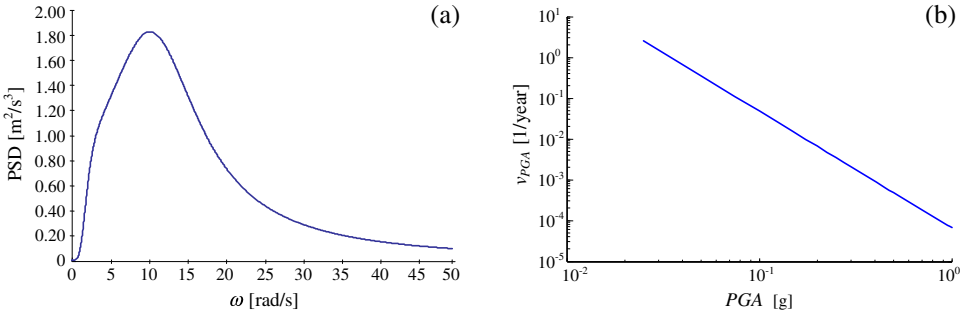

Figure 2. Input ground motion: (a) PSD function of the embedded stationary process and (b) site hazard curve.

PGA at the site is assessed empirically. A set of 5,000 synthetic stationary ground motion records are generated using the spectral representation method [35] on the basis of the PSD function given in Equation (8) with $S_0 = \bar{S}_0 = 1\ \mathrm{m}^2/\mathrm{s}^3$. Each ground motion realization is then modulated in time by using the function defined in Equation (7). The peak ground acceleration corresponding to $S_0 = \bar{S}_0 = 1\ \mathrm{m}^2/\mathrm{s}^3$, $PGA_{\bar{S}_0}$, is estimated as the mean of the *PGA*s of the sampled ground motion time histories. The values of S_0 corresponding to different values of *PGA* are obtained as follows:

$$S_0 = \left(\frac{PGA}{PGA_{\bar{S}_0}}\right)^2 \cdot \bar{S}_0 \tag{9}$$

In this study, the site hazard curve is expressed in the approximate form used by Cornell *et al.* [36], i.e.,

$$\nu_{IM}(im) = P\left[IM \geqslant im | 1\ \text{year}\right] = k_0 \cdot im^{-k_1} \tag{10}$$

in which k_0 and k_1 are parameters obtained by fitting a straight line through two known points of the site hazard curve plotted in logarithmic scale. For the applications presented in this paper, the site hazard curve is taken from Eurocode 8-Part 2 [4], assuming that for the site of interest, $PGA = 0.3g$ (where g is gravity constant) corresponds to a probability of being exceeded equal to 10% in 50 years (i.e., a return period of 475 years). Using $k_1 = 2.857$ [37], the site hazard curve becomes (see Figure 2(b))

$$\nu_{PGA}(pga) = 6.734 \cdot 10^{-5} \cdot pga^{-2.857} \tag{11}$$

The seismic model used here implies that all earthquakes affecting the considered adjacent structures are described by the same time-modulating and PSD functions, regardless of their magnitude and source distance. Although this assumption is not very realistic, it is adopted here only for the sake of simplicity and clarity and is not a limitation of the proposed framework. In fact, the design methodology introduced in this paper can employ different and more realistic seismic models, for example, obtained by (i) disaggregating into appropriate bins the seismic hazard with respect to source distance, magnitude, and epsilon [38]; (ii) associating to each bin a proper time-modulating and PSD function; and (iii) accounting for the different probabilities, corresponding to each bin, of one or more seismic events during the design lifetime of the structures.

3.2. Code procedure for the design of the critical separation distance between adjacent linear systems

The procedure reported in Lopez-Garcia and Soong [8] is adopted in this paper in order to illustrate the code approach for the determination of the CSD between adjacent buildings. This procedure involves generating a set of 5,000 artificial ground acceleration time histories consistent with the seismic hazard

DOI: 10.1002/eqe

level considered. In this study, the seismic intensity is represented by the *PGA* corresponding to a probability of exceedance of 10% in 50 years. For the sake of simplicity and in order to limit the computational cost of the analysis, the two adjacent buildings, referred to as buildings A and B, are modeled here as linear SDOF systems with natural periods equal to the periods of the first mode of vibration of each of the actual structural systems. Linear time-history analysis is employed to evaluate the 5,000 samples of the peak absolute displacement responses of buildings A and B ($U_{A,max}$ and $U_{B,max}$, respectively), corresponding to the 5,000 artificial ground motions previously generated. These sample peak absolute displacement responses are then averaged, and their sample means, $\bar{U}_{A,max}$ and $\bar{U}_{B,max}$, are combined following the ABS, SRSS, and DDC rules to derive the corresponding CSDs, which are assumed equal to the peak relative displacement $\bar{U}_{rel,max}$. The CSDs according to the ABS, SRSS, and DDC rules are denoted as ξ_{ABS}, ξ_{SRSS}, and ξ_{DDC}, respectively, and are computed as

$$\begin{aligned}\xi_{ABS} &= \overline{U}_{A,max} + \overline{U}_{B,max} \\ \xi_{SRSS} &= \sqrt{\overline{U}^2_{A,max} + \overline{U}^2_{B,max}} \\ \xi_{DDC} &= \sqrt{\overline{U}^2_{A,max} + \overline{U}^2_{B,max} - 2\cdot\rho\cdot\overline{U}_{A,max}\cdot\overline{U}_{B,max}}\end{aligned} \tag{12}$$

where ρ is the cross-correlation coefficient, given as [8]

$$\rho = \frac{8\cdot\sqrt{\zeta_A\cdot\zeta_B}\cdot\left(\zeta_A + \zeta_B\cdot\frac{T_A}{T_B}\right)\cdot\left(\frac{T_A}{T_B}\right)^{1.5}}{\left[1-\left(\frac{T_A}{T_B}\right)^2\right]^2 + 4\cdot\zeta_A\cdot\zeta_B\cdot\left[1-\left(\frac{T_A}{T_B}\right)^2\right]\cdot\left(\frac{T_A}{T_B}\right) + 4\cdot\left(\zeta_A^2+\zeta_B^2\right)\cdot\left(\frac{T_A}{T_B}\right)^2} \tag{13}$$

in which T_A and T_B are the natural vibration periods of buildings A and B, respectively; and ζ_A and ζ_B are the damping ratios of buildings A and B, respectively.

3.3. Critical separation distance for adjacent buildings modeled as linear SDOF systems: comparison of the three proposed algorithms

The first application example consists of the evaluation of the CSD between two adjacent buildings modeled as deterministic linear elastic SDOF systems with periods T_A and T_B and damping ratios $\zeta_A = \zeta_B = 5\,\%$. The CSD is estimated using the three different algorithms proposed for two different combinations of the natural periods of the adjacent systems, that is, (i) $T_A = 1.0$ s and $T_B = 0.5$ s, referred to as well-separated natural periods; and (ii) $T_A = 1.0$ s and $T_B = 0.9$ s, referred to as close natural periods. On the basis of previous results regarding the relative accuracy of different analytical approximations [17, 29], the cVM approximation is used in this study to compute the conditional pounding probability $P_{p|IM}(\xi)$ required to estimate $f(\xi)$ and $f'(\xi)$.

Table I reports the values of the design CSD, the number of analytical N_{an} and numerical N_{sim} computations of $P_p(\xi,t_L)$ required for convergence, the computational time, and the risk of pounding according to ISEE for the three algorithms and the two analysis cases considered. The algorithms stop when $|f(\xi)| \le 10^{-3}$. The calculations are performed using MATLAB [39] on a personal computer with an Intel Core i7 980 3.33 GHz processor (Intel Corp., Santa Clara, CA, USA) and 12.0-GB RAM.

Table I. Comparison of the three newly proposed design algorithms.

T_A = 1.0 s and T_B = 0.5 s					T_A = 1.0 s and T_B = 0.9 s				
Algorithm	CSD (m)	time (s)	N_{an}, N_{sim} (−)	P_p (ξ,t_L) (−)	Algorithm	CSD (m)	time (s)	N_{an}, N_{sim} (−)	P_p (ξ,t_L) (−)
AN	0.119	33	5,0	0.0908	AN	0.092	36	5,0	0.1129
HYB	0.116	982	6,2	0.1002	HYB	0.096	1498	6,2	0.0996
SIM	0.115	1362	5,3	0.1003	SIM	0.096	3621	5,5	0.1000

CSD, critical separation distance; AN, analytical; HYB, hybrid; SIM, simulation.

DOI: 10.1002/eqe

It is observed that $P_p(\xi,t_L)$ is very sensitive to small changes in ξ. The computational cost of the SIM algorithm is high and significantly larger than the computational cost of the AN and HYB algorithms. The AN algorithm is very fast and efficient; however, it is not as accurate as the SIM and HYB algorithms. The HYB algorithm yields accurate estimates of the separation distance at a small fraction of the computational cost of the SIM algorithm, because the analytical computation of $P_{p|IM}(\xi)$ is much faster than the computation of $P_{p|IM}(\xi)$ through the ISEE method. The similar accuracy of the SIM and HYB algorithms is expected because they both use ISEE for computing $P_{p|IM}(\xi)$ and they have the same termination rule, whereas the different computation of the gradient of $P_{p|IM}(\xi)$ affects only the computational cost of each iteration and the total number of iterations required to converge. It is noteworthy that, in both cases considered here, only one iteration of the HYB algorithm is needed to achieve the desired level of accuracy.

3.4. Critical separation distance for adjacent buildings modeled as linear SDOF systems: parametric analysis

The parametric analysis performed here compares the estimates of the CSD according to the code procedure (ξ_{ABS}, ξ_{SRSS}, and ξ_{DDC}) with the values of the CSD according to the HYB algorithm, that is, ξ^*_{HYB}, by considering (i) the effects of varying structural properties and (ii) the effects of varying site hazard. The HYB algorithm is stopped when $|f(\xi)| \le 5 \cdot 10^{-3}$. The cVM approximation is used here to compute the conditional pounding probability $P_{p|IM}(\xi)$ required to estimate $f(\xi)$ and $f'(\xi)$. The values ξ_{ABS}, ξ_{SRSS}, and ξ_{DDC} are generated by using a set of 5,000 records with a mean *PGA* equal to $0.3g$.

Figure 3 plots the values of ξ_{ABS}, ξ_{SRSS}, ξ_{DDC}, and ξ^*_{HYB} for different values of the ratio T_B/T_A and of T_A, in order to evaluate the effects of varying structural properties on the CSD.

In general, the CSD increases for increasing T_A. For a given period T_A, the CSD slowly increases when the ratio T_B/T_A increases from 0 to approximately 0.8 and rapidly decreases when T_B/T_A increases from 0.8 to 1. This behavior derives from the fact that when the ratio T_B/T_A approaches one, the two systems tend to vibrate in phase with a similar vibration period. In fact, in the limit case of $T_B/T_A = 1$, no separation distance would be required to avoid pounding because the two

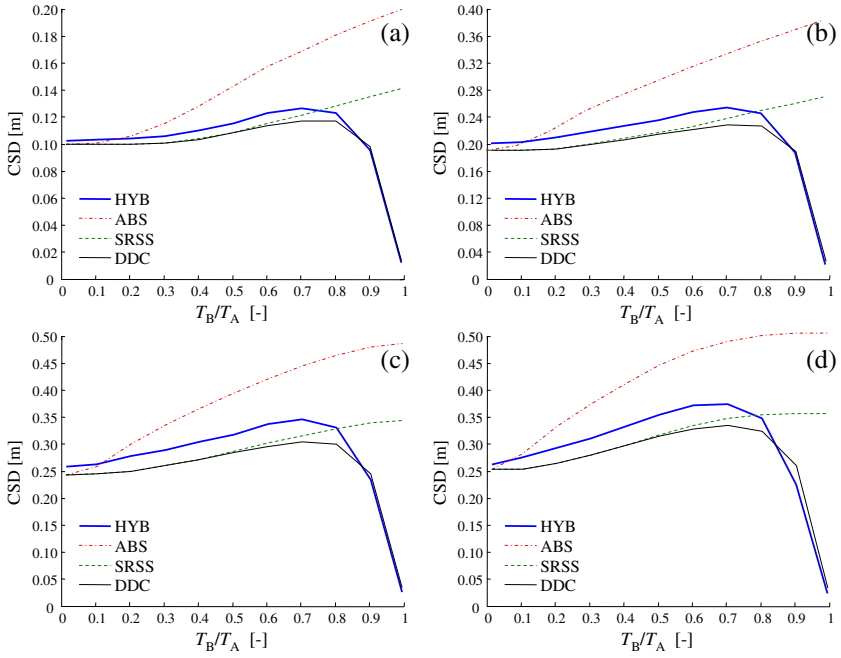

Figure 3. Critical separation distance (CSD) estimates for different ratio T_B/T_A: (a) $T_A = 1.0$ s, (b) $T_A = 2.0$ s, (c) $T_A = 3.0$ s, and (d) $T_A = 4.0$ s. HYB, hybrid; ABS, absolute sum; SRSS, square root of the sums of squares; DDC, double difference combination.

DOI: 10.1002/eqe

structures would vibrate exactly in phase. It is observed that the DDC rule provides values of the CSD close to those that are obtained applying the newly proposed procedure, particularly for large values of T_B/T_A. This phenomenon is due to the capability of the DDC rule to account for the phase difference in the displacement response of the two adjacent structures.

Figure 4 plots the values of the probability of pounding in 50 years corresponding to the separation distance, according to the code approach and the proposed algorithm, for the same values of the ratio T_B/T_A and of T_A considered in Figure 3.

It is observed that the pounding probability corresponding to the CSDs obtained using the HYB algorithm are very close to the target value of 10% for any value of T_B/T_A and of T_A. By contrast, the code approach provides inconsistent values of the pounding probability, which strongly depend on the ratio T_B/T_A and on T_A. The separation distance according to the code design approach provides nonconservative values of the risk for very low values of T_B/T_A, even when the ABS rule is employed.

The effects of varying site hazard are studied by considering different values of the parameter k_1 in Equation (10). In fact, the design of the CSD based on the seismic code procedure is performed for a single hazard level and ignores any other information regarding the seismic hazard of the buildings' site. Thus, this seismic code procedure gives CSD values that are independent of the shape of the hazard curve because they depend only on the value of the *PGA* corresponding to a target exceedance probability during the considered design life of the structure. This is in contrast with the proposed methodology, which can account for different shapes of the site hazard function. The design code procedure and the proposed HYB algorithm are applied to compute the CSD between adjacent buildings modeled as SDOF systems with $T_A = 2.0$ s and varying ratio T_B/T_A, using three different values of k_1 and a constant value $PGA = 0.30g$ that is assumed to have a probability of exceedance of 10% in 50 years. Figure 5(a) shows the CSD according to the seismic code procedure and HYB algorithm for $k_1 = 3.333$, $k_1 = 2.857$, and $k_1 = 2.222$, whereas Figure 5(b) plots the corresponding values of the probability of pounding.

In Figure 5(a), it is observed that only the CSD computed using the HYB algorithm varies with the shape of the hazard curve, whereas the CSDs computed using the ABS, SRSS, and DDC rules are independent of the hazard curve shape. Figure 5(b) shows that the proposed design method is able

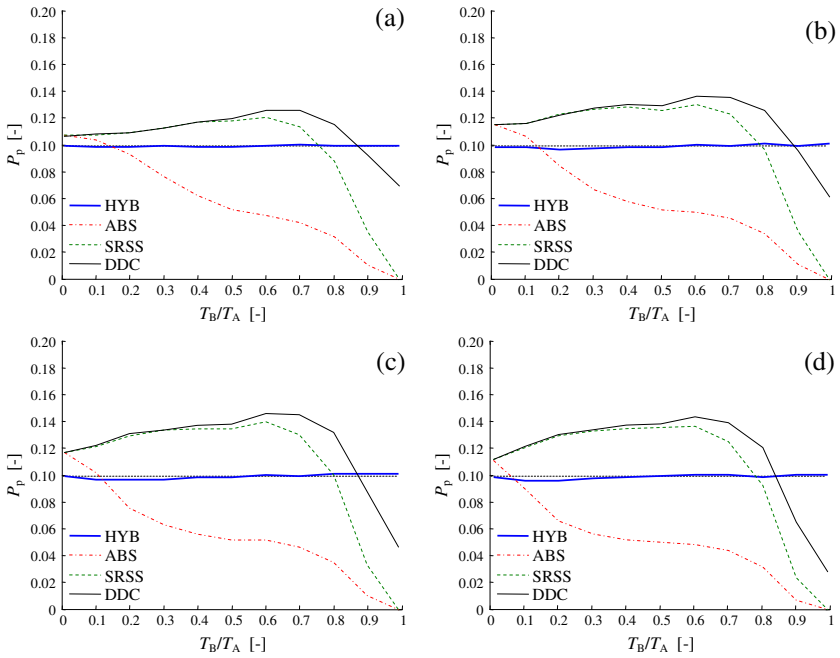

Figure 4. Probability of pounding in 50 years for different ratio T_B/T_A: (a) $T_A = 1.0$ s, (b) $T_A = 2.0$ s, (c) $T_A = 3.0$ s, and (d) $T_A = 4.0$ s. HYB, hybrid; ABS, absolute sum; SRSS, square root of the sums of squares; DDC, double difference combination.

DOI: 10.1002/eqe

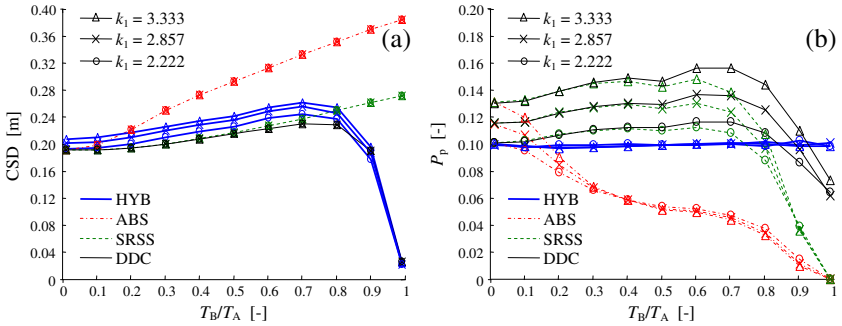

Figure 5. Effects of the hazard curve shape ($T_A = 2.0$ s): (a) design CSDs and (b) pounding probability in 50 years. CSD, critical separation distance ; HYB, hybrid; ABS, absolute sum; SRSS, square root of the sums of squares; DDC, double difference combination.

to provide CSDs corresponding to consistent values of the pounding probability that are independent of the properties of the structures and the site hazard. In fact, the HYB algorithm yields values of the probability of pounding very close to the target value of 10% for all the k_1 values considered, whereas the ABS, SRSS, and DDC rules provide CSDs for which the probability of pounding depends significantly on the shape of the site hazard curve.

3.5. Critical separation distance for adjacent buildings modeled as MDOF systems

The proposed design methodology is employed here to define the separation distance between two multistory adjacent buildings (Figure 6), whose properties are taken from Lin [40].

Building A is an eight-story shear-type building with constant inter-story stiffness $k_A = 628,801$ kN/m and floor mass $m_A = 454,545$ kg, whereas building B is a four-story shear-type building with constant inter-story stiffness $k_B = 470,840$ kN/m and floor mass $m_B = 454,545$ kg. A Rayleigh-type damping matrix $\mathbf{c_R}$ [41] is used to model the inherent viscous damping in the two systems. The matrix is built by assigning a damping factor $\zeta_R = 2\%$ to the first two vibration modes of each system vibrating alone. The fundamental vibration periods of the two buildings are $T_A = 0.915$ s and $T_B = 0.562$ s, respectively.

The seismic input model is the same as the one employed in the previous sections of this paper on SDOF systems. Five hundred ground motion records are employed in the Monte Carlo simulation required by the seismic design code procedure. The AN and HYB algorithms are employed in conjunction with the cVM approximation to determine the CSD. The AN algorithm requires 614 s

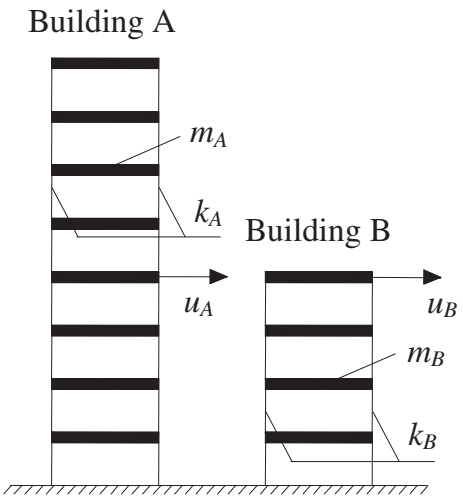

Figure 6. MDOF models of buildings A and B.

DOI: 10.1002/eqe

of analysis (of which 601 s are needed to calculate the closed-form spectral characteristics of the two models and 13 s are used to compute ξ^*_{AN}) to provide a CSD $\xi^*_{AN} = 0.166$ m. The HYB algorithm uses ξ^*_{AN} as the starting point and yields $\xi^*_{HYB} = 0.162$ m in 1641 s (614 s to obtain ξ^*_{AN} and 1027 s to obtain ξ^*_{HYB} afterward). The 50-year probabilities of pounding corresponding to ξ^*_{AN} and ξ^*_{HYB} are 9.09% and 9.94%, respectively. Also in this case involving the analysis of linear MDOF systems, the CSD obtained using the HYB algorithm corresponds to a pounding probability very close to the target probability value. Table II compares the values of the CSD obtained according to both the proposed algorithm and the seismic code rules, as well as their corresponding probability of pounding in 50 years and time of computation. Table II also reports the CSD values obtained using a simplified design approach suggested by Jeng *et al*. [5], which employs the seismic code rules in conjunction with the peak absolute displacements corresponding to the contribution of the first vibration mode only for each system. The computational cost associated with this simplified design approach is practically negligible under the assumption (commonly satisfied in practical design applications) that the peak absolute displacements can be obtained from an available displacement response spectrum.

It is observed that the use of the ABS rule yields a conservative value of the CSD, whereas the use of the SRSS and DDC combination rules yields CSDs that are nonconservative and correspond to a risk of pounding more than 50% higher than the target pounding probability. In this specific case, the simplified design approach yields values of the CSD that are very close to those obtained by rigorously following the code procedure, that is, by performing Monte Carlo simulation to compute the peak absolute displacements of the two MDOF systems. This observation suggests that the behavior of the two MDOF systems considered is dominated by their corresponding fundamental modes of vibration. The computational cost of the proposed design procedure is higher (by a factor larger than 2 for the AN algorithm and a factor approximately equal to 6 for the HYB algorithm) than the computational cost of the rigorous seismic design procedure. However, both the AN and HYB algorithms provide CSDs corresponding to pounding probabilities significantly closer to the target probability than the CSDs obtained from the seismic code procedure using any of the modal combination rules considered here.

In order to verify if the proposed design methodology can be further simplified and made computationally more efficient, the CSD is calculated with the HYB algorithm by using only the two fundamental vibration modes of the systems under study. This procedure is similar to simplified seismic design approaches that are allowed in some of the existing codes (e.g., in [4]). In this simplified approach, the CSD is computed on the basis of the relative displacement of the buildings corresponding to their first modes of vibration only, that is,

$$U_{rel}(t) = \gamma_A \cdot V_A \cdot Z_A(t) - \gamma_B \cdot V_B \cdot Z_B(t) \tag{14}$$

where γ_A and γ_B are the participation factors of the first modes of buildings A and B, respectively; V_A and V_B are the first-mode shape displacements at the pounding location (normalized by the first-mode displacement at the roof) of buildings A and B, respectively; and $Z_A(t)$ and $Z_B(t)$ are the time histories

Table II. CSD design results for the MDOF systems.

Method	CSD (m)	P_p (ξ,t_L) (%)	Time (s)
AN	0.166	9.09	614
HYB	0.162	9.94	1614
ABS	0.196	5.67	269
SRSS	0.139	15.47	269
DDC	0.139	15.62	269
ABS (1 mode)	0.198	5.42	—
SRSS (1 mode)	0.145	13.72	—
DDC (1 mode)	0.144	13.72	—

CSD, critical separation distance; AN, analytical; HYB, hybrid; ABS, absolute sum; SRSS, square root of the sums of squares; DDC, double difference combination.

DOI: 10.1002/eqe

of the generalized coordinate corresponding to the roof displacement according to the first mode of vibration of the two buildings and the specified seismic input.

The two equivalent SDOF systems corresponding to buildings A and B are characterized by the following properties: $T_{\mathrm{eq,A}} = 0.915$ s and $T_{\mathrm{eq,B}} = 0.562$ s (fundamental vibration periods), $m_{\mathrm{eq,A}} = 3{,}113{,}900$ kg and $m_{\mathrm{eq,B}} = 1{,}624{,}400$ kg (equivalent masses), $\zeta_{\mathrm{eq,A}} = \zeta_{\mathrm{eq,B}} = 2\%$ (equivalent damping ratio), and $\gamma_{\mathrm{A}} \cdot V_{\mathrm{A}} = 0.853$ and $\gamma_B \cdot V_{\mathrm{B}} = 1.241$. For this reduced-order model, the AN and HYB design algorithms yield $\xi^*_{\mathrm{AN}} = 0.166$ m and $\xi^*_{\mathrm{HYB}} = 0.161$ m, respectively, which correspond to a probability of pounding in 50 years equal to 9.15% and 9.96%, respectively. The computational time is reduced to 37 s for the AN algorithm (of which 24 s is needed to calculate the closed-form spectral characteristics of the two models and 13 s is used to compute ξ^*_{AN}) and 1,039 s for the HYB algorithm (of which 37 s is needed to compute ξ^*_{AN} and 1,002 s to obtain ξ^*_{HYB} afterward). This computational cost reduction is because the spectral characteristics and the probability of pounding according to the ISEE method are calculated for a 2-DOF system rather than for a 12-DOF system.

3.6. Critical separation distance for adjacent buildings modeled as nonlinear SDOF systems

In this section, the proposed CSD design methodology is applied to SDOF models with nonlinear hysteretic behavior. The same buildings used in the previous application are considered here. Their linear behavior is described by the same reduced-order SDOF models described earlier. A bilinear constitutive model with kinematic hardening describes the relationship between the inelastic restoring force and the displacement of the equivalent SDOF systems [9]. This constitutive model for building i (with $i = \mathrm{A, B}$) is defined by the yield force, $F_{\mathrm{y},i}$, and the ratio of the post-yield and initial stiffnesses, b_i, which is assumed equal to 0.05 for both models.

A parametric study is performed by introducing the force reduction factor, R_i ($i = \mathrm{A, B}$), which is defined as

$$R_i = \frac{m_{\mathrm{eq},i} \cdot S_a\left(T_{\mathrm{eq},i}, \zeta_{\mathrm{eq},i}\right)}{F_{\mathrm{y},i}} \quad (i = \mathrm{A,\ B}) \tag{15}$$

where $S_a(T_{\mathrm{eq},i},\zeta_{\mathrm{eq},i})$ is the spectral acceleration evaluated at the natural period of the equivalent SDOF, $T_{\mathrm{eq},i}$, with equivalent damping ratio, $\zeta_{\mathrm{eq},i}$, for $PGA = 0.3g$ (which is the seismic intensity level corresponding to a probability of exceedance equal to 10% in 50 years). The force reduction factor is varied from $R_i = 0$ to $R_i = 4$, with increments of 0.5 (for a total of nine discrete values of each force reduction factor), in order to describe a wide range of seismic behavior for the two systems. In particular, $R_i = 0$ corresponds to perfectly elastic behavior; $R_i = 1$ corresponds to buildings designed to respond elastically up to the seismic intensity of the design earthquake; and $R_i = 4$ corresponds to buildings designed to respond inelastically to the design earthquake with ductile behavior. For the $9 \times 9 = 81$ combinations of R_{A} and R_{B} considered, the CSD corresponding to a target probability of pounding of 10% in 50 years is obtained using the SIM algorithm in conjunction with crude Monte Carlo simulation. At each iteration of the SIM algorithm, 500 earthquake ground motion time histories are simulated on the basis of the earthquake ground motion model used in this study, and the peak relative displacements obtained from the corresponding 500 nonlinear time-history analyses are employed to estimate $f(\xi)$ and $f'(\xi)$. The iterative algorithm is terminated when $|f(\xi)| \leq 10^{-3}$. The CSD obtained using the method described earlier is denoted as $\xi^*_{\mathrm{nl,SIM}}$ and is a function of both R_{A} and R_{B}.

For the same combinations of R_{A} and R_{B}, the CSD corresponding to the application of the DDC rule, as modified by Kasai *et al*. [6, 9] to account for the nonlinear SDOF system behavior, is also computed. This modified DDC rule computes the CSD on the basis of Equations (12) and (13) and utilizes (for $i = \mathrm{A, B}$) an effective natural period, $T_{\mathrm{eff},i}$, and an effective damping ratio, $\zeta_{\mathrm{eff},i}$, instead of the elastic properties, $T_{\mathrm{eq},i}$ and $\zeta_{\mathrm{eq},i}$, for the two equivalent SDOF systems considered. These effective quantities, $T_{\mathrm{eff},i}$ and $\zeta_{\mathrm{eff},i}$, are computed using the empirical formulae presented by Kasai *et al*. [6] as applied by Lopez-Garcia [9]. They are functions of the average maximum ductility demands of each system, which are computed for $PGA = 0.3g$ through time-history simulation for varying R_{A} and R_{B} [9]. Thus, $T_{\mathrm{eff},i}$ and $\zeta_{\mathrm{eff},i}$ are functions of the corresponding R_i ($i = \mathrm{A, B}$), whereas

DOI: 10.1002/eqe

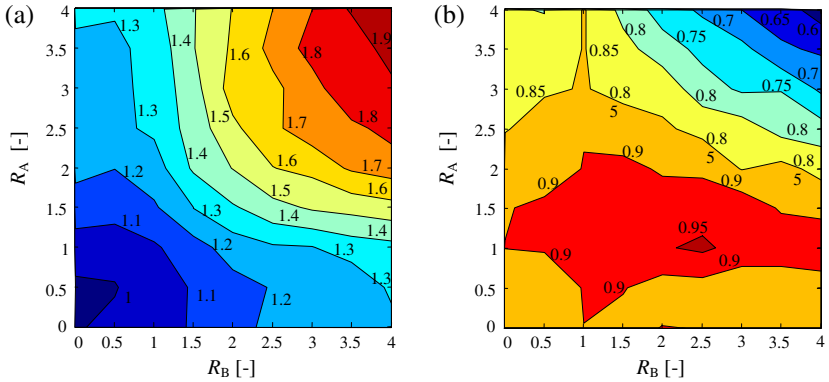

Figure 7. Critical separation distance for adjacent buildings modeled as nonlinear SDOF systems: (a) ratio of ξ^*_{lin} and $\xi^*_{nl,SIM}$, and (b) ratio of $\xi^*_{nl,DDC}$ and $\xi^*_{nl,SIM}$.

the separation distance between systems A and B is a function of both R_A and R_B. The CSD obtained using the modified DDC rule is denoted as $\xi^*_{nl,DDC}$.

Figure 7(a) shows the level curves, for varying R_A and R_B, of the ratio between $\xi^*_{lin} = 0.161$ m (which is the design CSD obtained by modeling the two systems as linear elastic and coincides with the solution ξ^*_{HYB} obtained in the previous example) and $\xi^*_{nl,SIM}$ (which is the design CSD obtained by modeling the two systems as nonlinear hysteretic equivalent SDOF systems). It is observed that the use of the linear behavior approximation for the two systems provides conservative values of the CSD, with an overestimation by a factor of almost 2 for $R_A = R_B = 4$. This phenomenon can be explained by observing that for increasing values of R_A and R_B, the two systems experience increasing period elongation and present higher hysteretic damping. Both effects promote an in-phase motion of the two systems, whereas higher hysteretic damping also reduces the displacement demand imposed on each system [5, 6, 9].

Figure 7(b) shows the level curves, for varying R_A and R_B, of the ratio between $\xi^*_{nl,DDC}$ and $\xi^*_{nl,SIM}$. It is observed that the modified DDC rule yields values of the separation distance that are significantly smaller than the distance $\xi^*_{nl,SIM}$, which corresponds to a probability of pounding of 10% in 50 years. For $R_A = R_B = 4$, the modified DDC rule underestimates the separation distance corresponding to the target reliability by a factor of about 40%, resulting in significantly nonconservative and unsafe results. In fact, the pounding probability in 50 years corresponding to the modified DDC rule results for $R_A = R_B = 4$ is equal to 55.58%, that is, more than 5.5 times higher than the target value.

4. CONCLUSIONS

This study presents a fully probabilistic performance-based methodology for determining the separation distance between adjacent buildings corresponding to a target level of the seismic pounding probability associated with the design life of the buildings. This separation distance is the solution of an inverse reliability problem in which the design input data are the characteristics of the buildings and the seismic excitation. The proposed methodology recasts the inverse reliability problem into a more manageable zero-finding problem. The approach developed in this paper allows the designer to control directly the pounding probability and thus represents a significant advancement when compared with current design code approaches and existing methods for the computation of the critical separation distance (CSD) between adjacent buildings, which lead to unknown safety levels. Additional advantages of the newly proposed methodology are the use of a continuum of hazard levels (instead of a single level of seismic hazard) and a more accurate representation of the pounding problem as a single-barrier reliability problem (instead of as a double-barrier reliability problem).

Three alternative iterative algorithms (referred to as AN, SIM, and HYB algorithms) are proposed for calculating the design separation distance and are specialized to the cases of linear elastic models subjected to Gaussian base excitations. The proposed specialized algorithms employ a combination

DOI: 10.1002/eqe

of analytical and simulation techniques and are characterized by different levels of precision and efficiency. The three proposed algorithms are compared in terms of accuracy and computational cost in the design of the separation distance between buildings modeled as linear SDOF systems with close and well-separated natural periods. It is found that the HYB algorithm provides highly accurate results (as accurate as the SIM algorithm and much more accurate than the AN algorithm) at a limited computational cost (i.e., larger than the computational cost of the AN algorithm but significantly smaller than the computational cost of the SIM algorithm).

The HYB algorithm is then employed in a parametric study assessing the dependence of the separation distance (and corresponding pounding probability) on the buildings' properties (represented by the natural periods of the two buildings) and the site hazard (represented by the slope of the linearized site hazard curve). By comparing the separation distances obtained using the proposed methodology with the HYB algorithm and the procedures suggested in modern seismic design codes based on approximate modal combination rules (i.e., the absolute sum (ABS), square-root-of-the-sums-of-squares (SRSS), and double difference combination (DDC) rule), the following observations are made: (i) the proposed design methodology provides design separation distances that correspond to pounding probabilities very close to the target pounding probability, independent of the structural properties and the site hazard; (ii) the application of the seismic code procedure results in separation distances that correspond to inconsistent and potentially nonconservative values of the probability of pounding; (iii) among the approximate modal combination rules, the DDC rule provides values of the separation distance that are overall in better agreement with the values obtained using the design methodology proposed in this paper, which presents a smaller variability in the corresponding probability of pounding; and (iv) the probability of failure in 50 years is very sensitive to variations in the separation distance, i.e., small variations in the separation distance can result in large variations in the probability of pounding.

The proposed probabilistic performance-based methodology is then applied to determine the design separation distance between buildings modeled as linear MDOF systems. Also in this case, the separation distance obtained using the proposed design methodology corresponds to a probability of pounding very close to the target probability. A simplified method to determine the design separation distance is then proposed on the basis of the use of the first vibration modes of the two buildings only. This simplified method appears promising because, in the application example considered here, it provides results that are very close to those obtained using the newly proposed general methodology, at a significantly lower computational cost.

Finally, the proposed methodology is applied to determine the design separation distance between two buildings modeled as equivalent SDOF systems with nonlinear hysteretic behavior for a wide range of nonlinearity levels. With reference to the specific application example considered here, it is observed that the use of the linear behavior approximation for the two systems provides conservative values of the CSD, whereas the use of existing simplified methods to approximately account for the buildings' nonlinear behavior can yield significantly nonconservative estimates of the separation distance.

The proposed methodology can be used to enhance current seismic code provisions that aim to mitigate the pounding risk and to calibrate appropriate safety factors for use with simpler methods of estimating the CSD between adjacent buildings. It can also be directly used for reliability-based design of the separation distance between adjacent buildings and is easily incorporated into modern performance-based engineering frameworks for structural design and assessment, such as the Pacific Earthquake Engineering Research Center framework.

ACKNOWLEDGEMENTS

The authors gratefully acknowledge support of this research by (i) the Louisiana Board of Regents (LA BoR) through the Pilot Funding for New Research (Pfund) Program of the National Science Foundation (NSF) Experimental Program to Stimulate Competitive Research (EPSCoR) under Award No. LEQSF(2011)-PFUND-225; (ii) the LA BoR through the Louisiana Board of Regents Research and Development Program, Research Competitiveness (RCS) subprogram, under Award No. LESQSF(2010-13)-RD-A-01; (iii) the Longwell's Family Foundation through the Fund for Innovation in Engineering Research (FIER) Program; and (iv) the LSU Council on Research through the 2009–2010 Faculty Research Grant Program. Any

DOI: 10.1002/eqe

opinions, findings, conclusions, or recommendations expressed in this publication are those of the authors and do not necessarily reflect the views of the sponsors.

REFERENCES

1. Building Center of Japan (BCJ). *Structural provisions for building structures*. Tokyo, Japan, 1997.
2. International conference of building officials (ICBO). *Uniform building code (UBC)*. Whittier, CA, USA, 1997.
3. Construction and Planning Administration Ministry of Interior. *Seismic Provisions. Taiwan Building Code (TPC)*. Taipei, Taiwan, 1997.
4. European Committee for Standardization. EN 1998–1:2004. *Eurocode 8—Design of Structures for Earthquake Resistance. Part 1: General Rules, Seismic Actions and Rules for Buildings*. European Committee for Standardization: Brussels, 2004.
5. Jeng V, Kasai K, Maison BF. A spectral difference method to estimate building separations to avoid pounding. *Earthquake Spectra* 1992; **8**(2):201–223.
6. Kasai K, Jagiasi RA, Jeng V. Inelastic vibration phase theory for seismic pounding. *Journal of Structural Engineering* 1996; **122**(10):1136–1146.
7. Penzien J. Evaluation of building separation distance required to prevent pounding during strong earthquake. *Earthquake Engineering and Structural Dynamics* 1997; **26**(8):849–858.
8. Lopez-Garcia D, Soong TT. Assessment of the separation necessary to prevent seismic pounding between linear structural systems. *Probabilistic Engineering Mechanics* 2009; **24**(2):210–223.
9. Lopez-Garcia D, Soong TT. Evaluation of current criteria in predicting the separation necessary to prevent seismic pounding between nonlinear hysteretic structural systems. *Engineering Structures* 2009; **31**(5):1217–1229.
10. Tubaldi E, Barbato M. Reliability-based assessment of seismic pounding risk between adjacent buildings. *Proceedings of 3rd International Conference on Computational Methods in Structural Dynamics and Earthquake Engineering* (*COMPDYN2011*), Corfu City, Greece, 2011.
11. Tubaldi E, Barbato M, Ghazizadeh S. A probabilistic performance-based risk assessment approach for seismic pounding with efficient application to linear systems. *Structural Safety* 2012; **36–37**:601–626 (Available from: http://dx.doi.org/10.1016/j.strusafe.2012.01.002).
12. Lin J-H. Separation distance to avoid seismic pounding of adjacent buildings. *Earthquake Engineering and Structural Dynamics* 1997; **26**(3):395–403.
13. Krawinkler H, Miranda E. Performance-based earthquake engineering. *Earthquake Engineering: From Engineering Seismology to Performance-Based Engineering*, Bozorgnia Y, Bertero VV (eds). CRC Press: Boca Raton, FL, 2004.
14. Collins KR, Wen YK, Foutch DA. Dual-level seismic design: a reliability-based methodology. *Earthquake Engineering and Structural Dynamics* 1996; **25**(12):1433–1467.
15. Wen YK, Foutch DA. Proposed statistical and reliability framework for comparing and evaluating predictive models for evaluation and design, and critical issues in developing such framework. *Technical Report SAC/BD-97/03*, SAC Joint Venture, 1997.
16. Hadjian AH. A general framework for risk-consistent seismic design. *Earthquake Engineering and Structural Dynamics* 2002; **31**(3):601–26.
17. Wen YK. Reliability and performance-based design. *Structural Safety* 2001; **23**(4):407–428.
18. Marano GC, Greco R. A performance-reliability-based criterion for the optimum design of bridge isolator. *ISET Journal of Earthquake Technology* 2004; **41**(2–4):261–276.
19. Li H, Foschi RO. An inverse reliability method and its applications. *Structural Safety* 1998; **20**(3):257–270.
20. Der Kiureghian A, Zhang Y, Li CC. Inverse reliability problem. *Journal of Engineering Mechanics* 1994; **120**(5):1154–1159.
21. Porter KA. An overview of PEER's performance-based earthquake engineering methodology. Proceedings, *Proceedings of the 9th International Conference on Application of Statistics and Probability in Civil Engineering* (*ICASP9*), San Francisco, California, 2003; 973–980.
22. Zhang Y, Acero G, Conte J, Yang Z, Elgamal A. Seismic reliability assessment of a bridge ground system. *Proceedings of the 13th World Conference on Earthquake Engineering*, Vancouver, Canada, 2004.
23. Barbato M, Conte JP. Spectral characteristics of non-stationary random processes: theory and applications to linear structural models. *Probabilistic Engineering Mechanics* 2008; **23**(4):416–426.
24. Barbato M, Vasta M. Closed-form solutions for the time-variant spectral characteristics of non-stationary random processes. *Probabilistic Engineering Mechanics* 2010; **25**(1):9–17.
25. Barbato M, Conte J. Structural reliability applications of nonstationary spectral characteristics. *Journal of Engineering Mechanics* 2011; **137**(5):371–382.
26. Au SK, Beck JL. First excursion probabilities for linear systems by very efficient importance sampling. *Probabilistic Engineering Mechanics* 2001; **16**(3):193–207.
27. Lin J-H, Weng C-C. Probability analysis of seismic pounding of adjacent buildings. *Earthquake Engineering and Structural Dynamics* 2001; **30**(10):1539–1557.
28. Ghazizadeh S, Barbato M, Tubaldi E. A new analytical solution of the first-passage reliability problem for linear oscillators. *Journal of Engineering Mechanics* 2011; **138**(6):695–706.

DOI: 10.1002/eqe

29. Ghazizadeh S. A study on the first-passage reliability problem and its application in earthquake engineering. *M.S. Thesis*, Civil and Environmental Engineering Department, Louisiana State University and A&M College, Baton Rouge, LA, USA, 2011.
30. Roberts JB, Spanos PD. *Random vibration and statistical linearization*. Dover Publications: New York, 2003.
31. Au SK, Beck JL. Estimation of small failure probabilities in high dimensions by subset simulation. *Probabilistic Engineering Mechanics* 2001; **16**(4):263–77.
32. Gill PE, Murray W, Wright MH. *Practical optimization*. Academic Press: London and New York, 1981.
33. Shinozuka M, Sato Y. Simulation of nonstationary random processes. *Journal of the Engineering Mechanics Division* 1967; **93**(1):11–40.
34. Clough RW, Penzien J. *Dynamics of Structures*. Mc.Graw Hill: New York, 1993.
35. Shinozuka M, Deodatis G. Simulation of stochastic processes by spectral representation. *Applied Mechanics Reviews* 1991; **44**(4):191–203.
36. Cornell C, Jalayer F, Hamburger R, Foutch D. Probabilistic basis for 2000 SAC federal emergency management agency steel moment frame guidelines. *Journal of Structural Engineering* 2002; **128**(4):526–32.
37. Lubkowski Z. *Deriving the Seismic Action for Alternative Return Periods Ac1cording to Eurocode 8*. (*14ECEE*), Ohrid: Macedonia, 2010.
38. Bazzurro P, Cornell CA. Disaggregation of seismic hazard. *Bulletin of the Seismological Society of America* 1999; **89**(2):501–20.
39. Math Works Inc. *MATLAB—High Performance Numeric Computation and Visualization Software*. *User's Guide*. Natick: MA, USA, 1997.
40. Lin JH. Evaluation of seismic pounding risk of buildings in Taiwan. *Chinese Institute of Engineers* 2005; **28**(5):867–72.
41. Chopra AK. *Dynamics of Structures: Theory and Applications to Earthquake Engineering* (2nd edn). Prentice Hall: Englewood Cliffs, NJ, 2001.

DOI: 10.1002/eqe